Heat Transfer Research 51(11):991–1005 (2020)

THE EFFECT OF UTILIZING Al_2O_3–SiO_2/DEIONIZED WATER HYBRID NANOFLUID IN A TUBE-TYPE HEAT EXCHANGER

Ataollah Khanlari

University of Turkish Aeronautical Association, Faculty of Engineering, Department of Mechanical Engineering, Ankara, Turkey, E-mail: akhanlari@thk.edu.tr, ata_khanlari@yahoo.com

Original Manuscript Submitted: 3/6/2020; Final Draft Received: 5/29/2020

One of the significant issues in energy conversion systems is efficient heat transfer which is generally done by heat exchangers (HEs). Different ways have been utilized to increase the performance of HEs. One of these ways for enhancing heat transfer rate is using a nanofluid. In this experimental work, the effect of utilizing Al_2O_3–SiO_2/deionized water hybrid nanofluid at various particle ratios on the efficiency of parallel flow tube-type heat exchanger (PFTHE) and counterflow tube-type heat exchanger (CFTHE) has been investigated experimentally. Hybrid nanofluids have been made by dispersing Al_2O_3–SiO_2 nanoparticles in water at weight concentrations of 0.5, 1, and 1.5%. In addition, to avoid sedimentation and also to improve stability of hybrid nanofluids, surfactant has been added into the nanofluid. The tests have been performed in different configurations to illustrate the effect of utilizing hybrid-type nanofluids. Using Al_2O_3–SiO_2/deionized water hybrid nanofluid led to a maximum enhancement of 25%, 60%, and 67% of the overall heat transfer coefficient at 0.5%, 1%, and 1.5% nanoparticle ratio, respectively.

KEY WORDS: *hybrid nanofluid, Al_2O_3–SiO_2, heat exchanger, tube-type, heat transfer*

1. INTRODUCTION

In the past decades, rising world population has caused an increase in the global energy consumption. So, developing new efficient energy systems is inevitable due to limited fossil resources and increasing air pollution. One of the significant issues in energy conversion systems is efficient heat transfer that is generally done by using HEs (Afshari et al., 2017; Variyenli, 2019). Several types of HEs are usually used in different industries. The thermal efficiency of HEs can be enhanced by applying different methods such as adding fins and ribbed surfaces. Moreover, utilizing nanofluids instead of traditional heat transfer working fluids is an efficient method to rise the thermal efficiency of HEs. The nanofluids are suspensions of nanoparticles in the base working fluid that can increase the efficiency due to their superior thermophysical characteristics in comparison with conventional working fluids (Ağbulut and and Sarıdemir, 2018; Kaya et al., 2019; Akhlaghi et al., 2018; Ağbulut et al., 2020). The performance of utilizing nanofluids in HEs belongs to both nanofluid properties and geometrical parameters of the heat exchanger used. Also, it should be indicated that the thermal behavior of nanofluids belongs to different parameters like nanoparticle type, nanoparticle size, nanoparticle shape, ratio of nanoparticles, surfactant type, and base fluid properties (Badali et al., 2019, 2020; Sözen et al., 2018, 2019).

Further enhancement in thermal performance of nanofluids can be achieved by mixing two or more various particles in the base working fluids that are known as hybrid nanofluids. One type of nanoparticles cannot have all desired properties. Therefore, hybrid nanofluids are suitable to utilize as these nanofluids supply enhanced thermal behavior due to synergetic effect (Sajid and Ali, 2018). In some studies, it has been indicated that hybrid nanofluids illustrated better thermal behavior than the nanofluids that include one type of nanoparticles (Saba et al., 2019; Giwa et al., 2020; Zufar et al., 2020).

There are lots of researches which investigated thermal behavior of hybrid-type nanofluids. Soylu et al. (2018) analyzed the influence of adding various nanoparticles, including TiO_2, TiO_2 doped with Ag, and TiO_2 doped with Cu, to ethylene glycol–water as a base fluid on the performance of automobile radiator. Their experimental results indicated that the nanofluid containing TiO_2 doped with Ag exhibited the best thermal performance in comparison with other nanofluids. Karimi and Afrand (2018) numerically analyzed the performance of MgO–MWCNTs/eth-

NOMENCLATURE

A	heat transfer area, m^2	**Greek Symbols**	
c_p	specific heat capacity, kJ/kg·K	ΔT_{ln}	logarithmic mean temperature difference, K
C	heat capacity rate, W/K		
$\dot{E}_{loss}$	exergy loss, W	ε	heat exchanger effectiveness
e	dimensionless exergy loss		
$\boldsymbol{h}$	heat transfer coefficient, $W/m^2 \cdot K$	**Subcripts**	
lpm	liter per minute		
$\dot{m}$	mass flow rate, kg/s	c	cold
$\dot{Q}$	heat transfer rate, W	e	environment
s	specific entropy, J/kg K	h	hot
T	temperature, K	i	inner
U	overall heat transfer coefficient, $W/m^2 \cdot K$	in	inlet
		o	outer
W_R	total uncertainty, %	out	outlet
w_1, w_2, and w_3	uncertainties in the independent variables	I	function uncertainty
		T	total

ylene glycol hybrid nanofluid in an air-cooled HE. They reported that using this hybrid nanofluid can improve the efficiency up to 10%. Hormozi et al. (2016) experimentally examined the influence of utilization of alumina–silver/water hybrid nanofluid on thermal efficiency of helical coil HE. Also, they investigated the effect of surfactant type. Their findings showed that this hybrid nanofluild can enhance the thermal performance up to 16%. Bahiraei et al. (2019) numerically analyzed the effect of using hybrid nanofluids containing graphene nanoplatelet–platinum in tube-type heat exchangers with inserted ribs. Their outcomes demonstrated that increasing the nanoparticle ratio and rib height can increase heat transfer in a heat exchanger.

Table 1 summarizes some studies in the literature that utilized Al_2O_3/water and SiO_2/water nanofluids in different HEs. As it can be seen, utilizing these two nanofluids separately enhanced the thermal efficiency in various heat exchangers. In this study it is proposed to improve the thermal efficiency of tube-type heat exchanger (THE) by utilizing Al_2O_3–SiO_2/deionized water hybrid nanofluid, since one type of nanoparticles cannot have all desired properties. In this regard, Al_2O_3–SiO_2/deionized water hybrid-type nanofluid has been tested in the tube-type heat exchanger in various flow modes. In addition, the optimum particle concentration for Al_2O_3–SiO_2/deionized water hybrid nanofluid has been investigated. The major steps of this study are illustrated in Fig. 1.

2. MATERIAL AND METHODOLOGY

2.1 Test Setup

The schematic view of the test setup used in the present work is illustrated in Fig. 2. Two various fluid circuits are available in the test setup consisting of cold and hot loops. In the present work, Al_2O_3–SiO_2/water nanofluid has been tested in hot fluid loop of the HE. Hot fluid (Al_2O_3–SiO_2/water) is warmed by using two electrical resistances which were located inside a hot fluid reservoir and then circulated into a hot side by a circulation pump. In the experimental apparatus to control the hot fluid level inside the tank a bullseye has been utilized. Moreover, to control unexpected jump in pressure a regulator has been mounted in the system. Two flowmeters have been

TABLE 1: Some studies of Al_2O_3/water and SiO_2/water utilization in different types of heat exchangers

Reference	Nanofluid	Type of Heat Exchanger	Concentration	Average Size of Particles (nm)	Main Findings
Sonawane et al. (2013)	Al_2O_3/water	Concentric type	2 and 3 vol.%	20	Maximum 47.36% increment in the heat transfer coefficient
Akyürek et al. (2018)	Al_2O_3/water	Concentric type	0.4, 0.8, 1.2, and 1.6 vol.%	40–47	Total heat transfer coefficient raised in the range of 15.98–36.58%
Mansoury et al. (2020)	Al_2O_3/water	Double pipe	0.2, 0.5, and 1 vol.%	20	Maximum 60% increment in heat transfer coefficient
Anoop et al. (2013)	SiO_2/water	Plate type	2–6 wt.%	20	Maximum 7% increment in heat transfer coefficient
Shahrul et al. (2016)	Al_2O_3/water and SiO_2/water	Shell-and-tube	0.5 vol.%	10–20	Heat transfer coefficient raised as 26% and 12% using Al_2O_3/water and SiO_2/water, respectively
Ozdemir and Ergun (2019)	Al_2O_3/water	Plate type	2 wt.%	100	Thermal efficiency improved as16%
Kabeel et al. (2013)	Al_2O_3/water	Plate type	1–4 vol.%	47	13% improvement in heat transfer coefficient

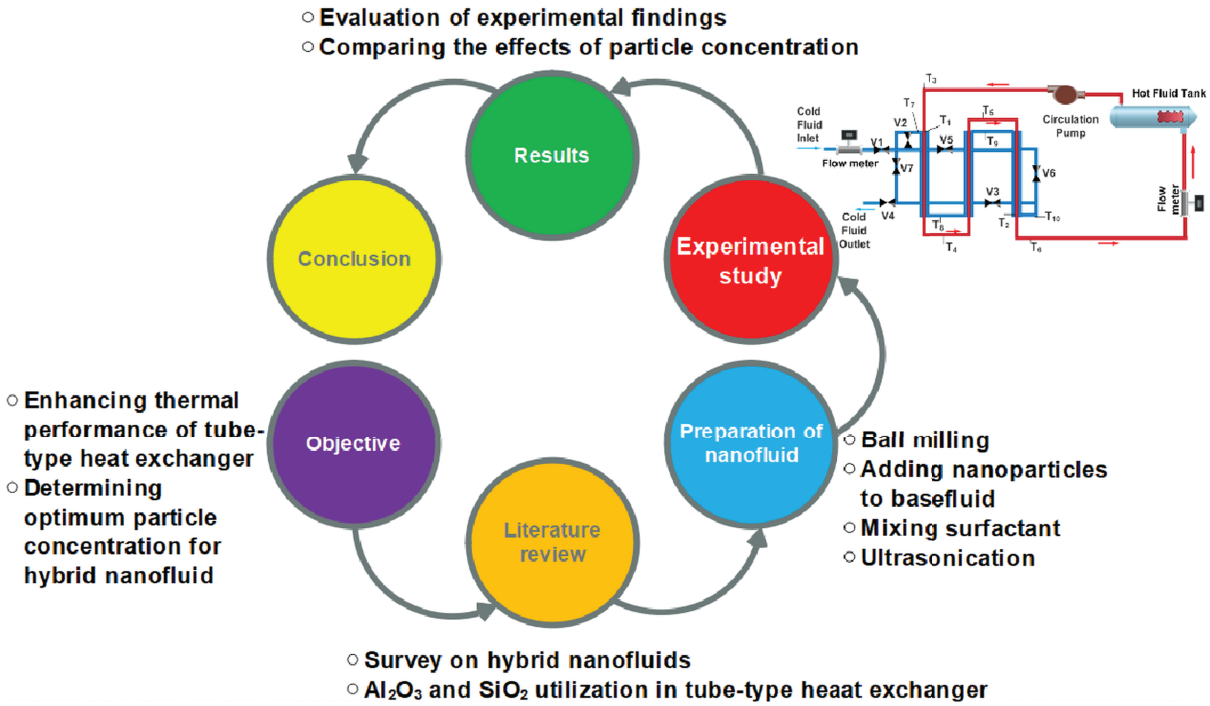

FIG. 1: The major steps of this study

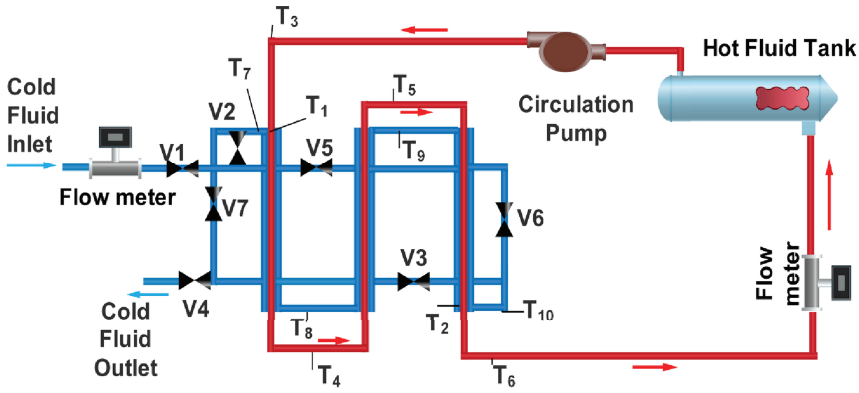

FIG. 2: Schematic view of the experimental setup

used in the experimental apparatus to set the flow rate in the cold and hot sides. In the experimental apparatus ten thermocouples were utilized to record temperature in two fluid loops. The properties of the utilized instruments in the test rig are listed in Table 2. In the tube-type heat exchanger section of setup, cold fluid flows over the exterior tube and hot fluid flows over the inner tube. Adjustable design of the experimental apparatus allows one to use the HE in parallel flow and counterflow modes by adjusting the valves which were mounted in the setup. The hot fluid is warmed up inside the reservoir and then is transferred to the HE and releases its thermal energy to the cold fluid which flows over the exterior tube of the HE. The cold fluid is poured from the system after gaining thermal energy in the heat exchanger.

TABLE 2: The properties of the utilized equipment in the test rig

Equipment	Properties
Cold loop flowmeter (g/s)	4–50
Hot loop flowmeter (lpm)	1–10
Hot loop interior radius (cm)	0.395
Hot loop exterior radius (cm)	0.475
Cold loop interior radius (cm)	0.555
Cold loop exterior radius (cm)	0.635
Interior heat transfer area (cm^2)	260
Exterior heat transfer area (cm^2)	310
Mean heat transfer area (mm^2)	288
Total flow area (m^2)	0.49
Pump head (mSS)	1.5
Heat supply (W)	3000
Thermocouple	J
Sensitivity of temperature indicator (^oC)	0.1

2.2 Preparation Procedure for the Nanofluid

In the first step of making nanofluid, to acquire homogeneous Al_2O_3 and SiO_2 nanoparticles and to decrease the size of particles, a ball milling process has been carried out for 8 h. In the second step, hybrid nanofluids at weight concentrations of 0.5, 1, and 1.5% have been made by dispersing the mixture of Al_2O_3 and SiO_2 nanoparticles in deionized water as the base fluid. In addition, to avoid precipitation and also to stabilize the hybrid nanofluids, sodium dodecyl benzene sulfonate (SDBS) surfactant has been added to the nanofluid by consulting related studies in the literature (Çiftçi and Sözen, 2020; Khanlari et al., 2020). A mixing surfactant enhances wetting capability of the prepared nanofluids and also decreases the surface tension. In addition to using the surfactant, an ultrasonic bath has been utilized to obtain more stable nanofluids. The prepared hybrid nanofluids are shown in Fig. 3.

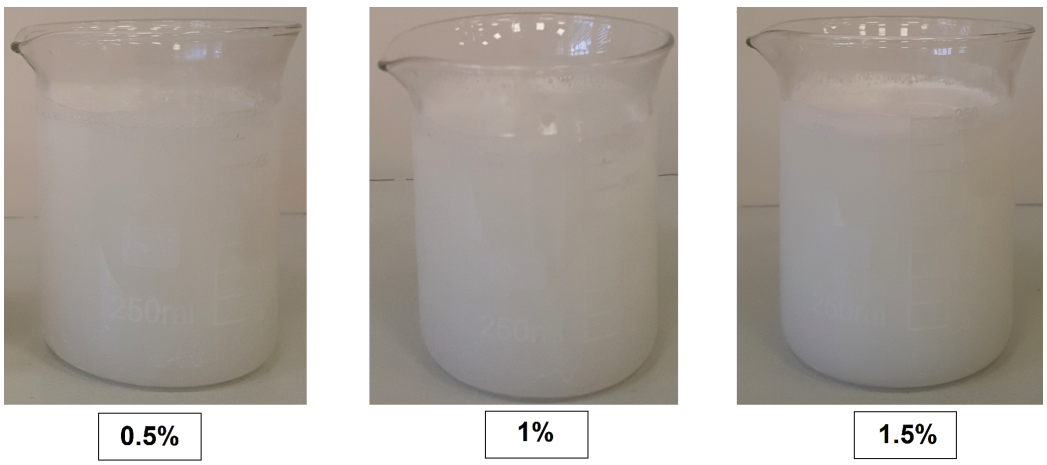

FIG. 3: Prepared hybrid nanofluids

After preparing hybrid nanofluids, the thermophysical characteristics of them have been determined. The densities of hybrid nanofluids have been achieved by getting weight of a certain volume of nanofluids under environmental conditions by using an analytical balance. The viscosities of prepared hybrid nanofluids have been obtained by an AND SV-10 viscometer. Moreover, the specific heat capacity of prepared samples has been determined utilizing the differential scanning calorimetry technique. In this context, a Perkin Elmer brand DSC apparatus was employed to get the heat capacity of Al_2O_3–SiO_2/water in different concentrations.

2.3 Experiments

Water has been tested on the hot side of the HE in the first step of the tests. Then the performance tests of prepared Al_2O_3–SiO_2/deionized water nanofluids have been conducted and compared with deionized water. The performance tests were done at various flow rates (3–9 lpm) to determine the impact of utilizing this hybrid nanofluid and also to illustrate the influence of particle concentration. The flow rate of cold fluid was kept constant (10 g/s). In order to get more accurate outcomes each experiment was repeated three times and the obtained mean values were employed in the analysis.

2.4 Theoretical Calculations

The heat transferred in a HE can be expressed as the heat gained by the cold loop ($\dot{Q}_c$) or the heat released by the hot loop ($\dot{Q}_h$). The heat released by the hot loop of the THE can be obtained as

$$\dot{Q}_h = \dot{m}_h c_{p,h}(T_3 - T_6). \tag{1}$$

In addition, the heat achieved by the cold loop of the THE can be expressed as

$$\dot{Q}_c = \dot{m}_c c_{p,c}(T_7 - T_{10}). \tag{2}$$

The highest thermal performance can be achieved when the heat transferred in the hot loop is equal to the heat transferred in the cold loop by assuming the thermal energy transfer from the internal fluid (hot loop) to external fluid (cold loop), by ignoring the resistance in the transfer area, and neglecting measuring errors:

$$\dot{Q}_c = \dot{Q}_h. \tag{3}$$

The effectiveness of HE as a crucial indicator in evaluating the performance of HE can be calculated by the following equation:

$$\varepsilon = \frac{\dot{Q}}{\dot{Q}_{\max}} = \frac{C_h(T_{h,i} - T_{h,o})}{C_{\min}(T_{h,i} - T_{c,i})} = \frac{C_c(T_{c,o} - T_{c,i})}{C_{\min}(T_{h,i} - T_{c,i})}. \tag{4}$$

Here C_c and C_h are the heat capacity of cold fluid and hot fluid, respectively, that can be expressed as

$$C_h = \dot{m}_h c_{p,h}, \tag{5a}$$

$$C_c = \dot{m}_c c_{p,c}. \tag{5b}$$

The thermal energy transferred between the tube surface area and the fluid flowing along the tube can be achieved as

$$\dot{Q} = hA\Delta T_{\ln}, \tag{6}$$

where h represents the coefficient of heat transfer (HTC) between the flowing fluid and the interior area of the tube, A is the area, and $\Delta T_{\ln}$ shows the logarithmic mean temperature difference and can be expressed as (Sözen et al., 2016a)

$$\Delta T_{\ln} = \frac{\Delta T_{\text{inlet}} - \Delta T_{\text{outlet}}}{\ln\left(\frac{\Delta T_{\text{inlet}}}{\Delta T_{\text{outlet}}}\right)}. \tag{7}$$

By rearranging the mentioned equations, the thermal energy removed from the hot loop can be achieved as follows:

$$\dot{Q}_h = \frac{h_h A_i[(T_3 - T_1) - (T_6 - T_2)]}{\ln\left(\frac{T_3 - T_1}{T_6 - T_2}\right)}. \tag{8}$$

The HTC in the hot loop of the tube-type exchanger can be calculated by Eq. (8). Moreover, the rate of heat transferred on the cold side of the tube-type heat exchanger can be calculated by the following equation:

$$\dot{Q}_c = \frac{h_c A_o[(T_1 - T_7) - (T_2 - T_{10})]}{\ln\left(\frac{T_1 - T_7}{T_2 - T_{10}}\right)}. \tag{9}$$

The overall heat transfer coefficient (OHTC) as another crucial indicator in the HE performance can be obtained as (Sözen et al., 2016b)

$$\dot{Q}_{\text{hot}} = A_T U \left[\frac{(T_3 - T_7) - (T_6 - 10)}{\ln\left(\frac{T_3 - T_7}{T_6 - 10}\right)}\right]. \tag{10}$$

Exergy can be expressed as the maximum work that can be obtained in the theory in a reversible process under certain environmental conditions. In this context, the reference environmental conditions must be determined to evaluate exergy. In this study, the reference ambient temperature is 20°C. Two types of losses can occur in a HE including the effect of temperature difference and pressure drop. However, in this study, exergy analysis has been performed by considering heat transfer irreversibility and ignoring the pressure drop factor. So, exergy loss in THE can be expressed as the total amount of exergy losses in hot and cold flows (Heyhat et al., 2018):

$$\dot{E}_{\text{loss}} = \dot{E}_{\text{loss},h} + \dot{E}_{\text{loss},c}. \tag{11}$$

Equation (11) can be rewritten as follows:

$$\dot{E}_{\text{loss}} = \dot{m}_h T_e \left(s_{h,\text{out}} - s_{h,\text{in}}\right) + \dot{m}_c T_e (s_{c,\text{out}} - s_{c,\text{in}}). \tag{12}$$

The entropy change can be defined using the following equation by assuming fixed thermophysical specifications for the utilized working fluids:

$$s_{\text{out}} - s_{\text{in}} = c_p \ln \frac{T_{\text{out}}}{T_{\text{in}}}. \tag{13}$$

So, Eq. (12) can be rearranged as follows:

$$\dot{E}_{\text{loss}} = T_e \dot{m}_h c_p \ln\left(\frac{T_{h,\text{out}}}{T_{h,\text{in}}}\right) + T_e \dot{m}_c c_p \ln\left(\frac{T_{c,\text{out}}}{T_{c,\text{in}}}\right). \tag{14}$$

By supposing a reference for fluid with peak temperature, in other words the fluid with lowest heat capacity rate, in the tube-type HE the dimensionless exergy loss can be obtained as follows:

$$e = \frac{\dot{E}_{\text{loss}}}{T_e C_{\min}}, \tag{15}$$

where $C_{\min}$ illustrates the lowest heat capacity rate and also T_e denotes the environment temperature.

2.5 Uncertainty Analysis

Throughout the test procedure, flow rates and temperature values were obtained by appropriate measuring devices. Uncertainty evaluation is a helpful means for obtaining uncertainties and also for evaluating the empirical outcomes. Experimental uncertainties may arise from measuring device specifications, device calibration, connection types of utilized devices, and also from experimental conditions (Karagöz et al., 2017). The total uncertainty in the test process can be obtained by Eq. (16) (Karagöz et al., 2020). The specifications of utilized measurement device and their uncertainties are given in Table 3. The uncertainties obtained in this study are in good agreement with results of similar studies in the literature (Afshari et al., 2019; Khanlari et al., 2020)

$$W_{\mathrm{R}} = \left[\left(\frac{\partial R}{\partial x_1} w_1\right)^2 + \left(\frac{\partial R}{\partial x_2} w_2\right)^2 + \ldots + \left(\frac{\partial R}{\partial x_n} w_n\right)^2\right]^{1/2}. \tag{16}$$

3. RESULTS AND DISCUSSION

In this section, the main outcomes of experimental study have been illustrated and explained in detail. An average size of Al_2O_3 and SiO_2 nanoparticles is 78 nm and 35 nm, respectively. Also, the thermophysical specifications of Al_2O_3–SiO_2/deionized water hybrid nanofluids at different concentrations are illustrated in Table 4.

The performance tests of hybrid nanofluids have been done at different fluid flow rates to determine the influence of using hybrid-type nanofluids on the hot side of tube-type heat exchanger. The change in OHTC with flow rate of hot fluid in PFTHE for water and hybrid nanofluids is shown in Fig. 4. As is seen, OHTCs of hybrid nanofluids are higher than that of water at all flow rates. The highest improvement in OHTC was obtained as 25%, 60%, and 67% at 0.5%, 1%, and 1.5% nanoparticle concentration, respectively. In addition, an increment in OHTC of PFTHE was obtained in the range of 12–25%, 22–60%, and 27–67% by using Al_2O_3–SiO_2 nanoparticles at 0.5%, 1%, and 1.5% concentration, respectively.

The change in the HTC on the hot side with respect to the flow rate of hot side in PFTHE is illustrated in Fig. 5. The obtained HTC of Al_2O_3–SiO_2/deionized water nanofluid is high in comparison with HTC of water at every flow rate, with a peak enhancement of 32%, 39%, and 56% at 0.5%, 1%, and 1.5% nanoparticle concentration, respectively. Also, improvement in HTC of PFTHE was achieved in the range of 11–32%, 21–39%, and 31–56% by using Al_2O_3–SiO_2 nanoparticles at 0.5%, 1%, and 1.5%, respectively. As is clearly seen from the figure, HTC is increased by increasing the flow rate for hybrid nanofluids and also for deionized water. In the present work, HTC on the hot side in PFTHE was achieved in the range of 6700–15,800 W/m^2·K. In a research done by

TABLE 3: Measurement device specifications

Device	Quantity	Range	Accuracy	Uncertainty
Thermocouples	10	0–350°C	0.5°C	± 0.588°C
Cold loop flowmeter	1	4–50 g/s	± 5%	± 5.36%
Hot loop flowmeter	1	1–10 lpm	± 5%	± 5.13%

TABLE 4: Thermophysical specifications of prepared nanofluids

Fluid	Viscosity (mPa·s)	Density (kg/m^3)
Deionized water	0.89	998
Al_2O_3/SiO_2 (0.5%)	0.90	1003
Al_2O_3/SiO_2 (1%)	0.91	1005
Al_2O_3/SiO_2 (1.5%)	0.93	1009

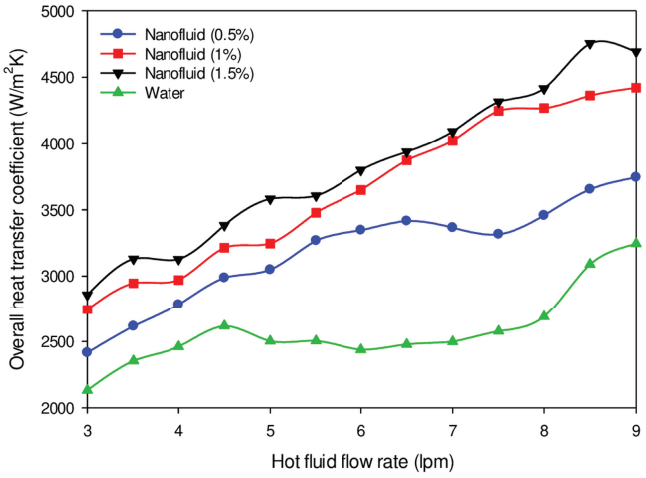

FIG. 4: OHTC change with respect to the flow rate in PFTHE

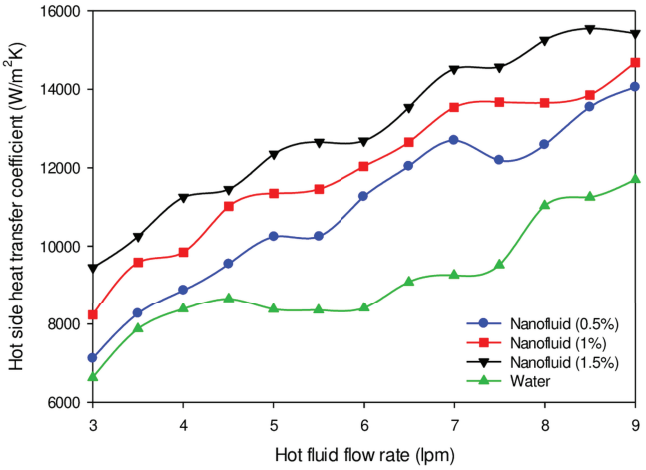

FIG. 5: Change in HTC of the hot side with respect to the flow rate in PFTHE

Khanlari et al. (2020), kaolin/water nanofluid was tested in a tube-type HE and HTC on the hot side was reported to be in the range 6000–16,000 W/m^2·K. In addition, in a study performed by Sözen et al. (2016a), fly ash/water was utilized in a tube-type HE and HTC on the hot side was achieved between 6000–17,000 W/m^2·K. As it is seen, the HTC obtained in this study is in good agreement with that of similar studies.

Figure 6 shows variation in HTC of the cold side with respect to the flow rate in PFTHE. The obtained cold side HTC for hybrid nanofluids is higher in comparison with that of water at all flow rates, with a maximum increment of 9%, 12%, and 19% at 0.5%, 1%, and 1.5% nanoparticle concentration, respectively. However, increment in HTC of the cold side of PFTHE was achieved in the range of 5–9%, 8–12%, and 12–19% by using Al_2O_3–SiO_2 nanoparticles at 0.5%, 1%, and 1.5% concentration, respectively. In a study performed by Khanlari et al. (2020), a maximum HTC enhancement of 19% was achieved on the cold side of THE by utilizing kaolin/water nanofluid including 2% particle concentration.

As mentioned above, the experiments have been done in two different modes of HE including parallel flow and counterflow. The change in OHTC with hot fluid flow rate in counterflow tube-type HE (CFTHE) for water and hybrid nanofluids is illustrated in Fig. 7. As is clearly seen from the figure, OHTC is improved by utilizing Al_2O_3–SiO_2/deionized water nanofluid in the hot circuit of CFTHE. A maximum increment in OHTC was obtained

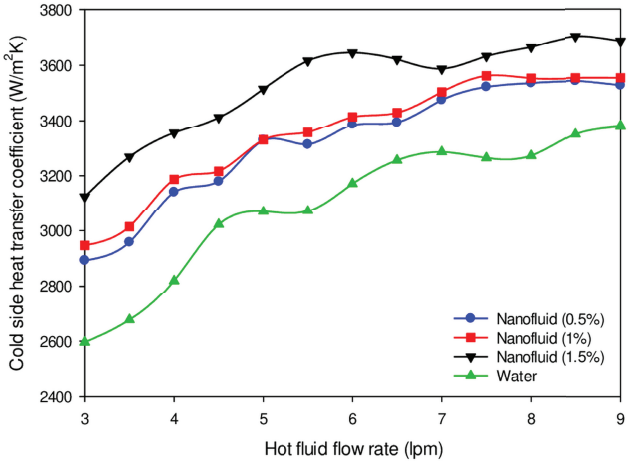

FIG. 6: Change in HTC of the cold side with respect to the flow rate in PFTHE

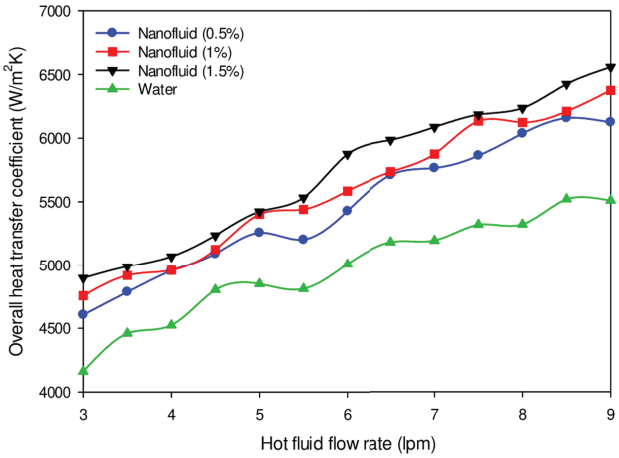

FIG. 7: Change in OHTC with respect to the flow rate in CFTHE

as 13%, 17%, and 20% at 0.5%, 1%, and 1.5% nanoparticle concentration, respectively, while the increment in OHTC of PFTHE was achieved in the range of 9–13%, 11–17%, and 12–20% by using Al_2O_3–SiO_2 nanoparticles at 0.5%, 1%, and 1.5% concentration, respectively. The obtained OTHC for CFTHE is in the range of 4200–6500 W/m^2·K. Khanlari et al. (2020) achieved OHTC in the range of 4200–6100 W/m^2·K in a counterflow THE by utilizing kaolin/water nanofluid. Also, Sözen et al. (2016b) achieved OHTC between 2000–3800 W/m^2·K in a counterflow THE by utilizing Al_2O_3 and fly ash/water nanofluids.

The variation of the HTC of hot fluid in CFTHE is shown in Fig. 8. The HTC of Al_2O_3–SiO_2/water nanofluids is improved at every flow rate, with a peak increment of 12%, 27%, and 39% at 0.5%, 1%, and 1.5% nanoparticle concentration, respectively. In addition, enhancement in HTC of hot fluid in CFTHE was achieved in the range of 7–12%, 10–27%, and 21–39% by using Al_2O_3–SiO_2 nanoparticles at 0.5%, 1%, and 1.5%, respectively. As is seen in the figure, the HTC of the hot side increased by rising the flow rate of hot fluid for hybrid nanofluids and also for deionized water.

Figure 9 shows the variation in HTC of the cold side with respect to the flow rate of hot fluid in CFTHE. The attained cold side HTC for hybrid nanofluids is higher in comparison with that of the water at every flow rate. Improvement in HTC of CFTHE was achieved in the range of 2–5%, 3.4–6.5%, and 6.5–13% by using Al_2O_3–SiO_2

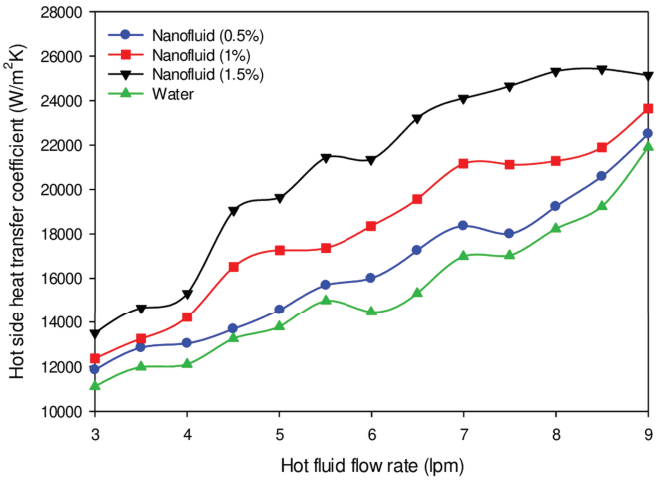

FIG. 8: Change in HTC of the hot side with respect to the flow rate in CFTHE

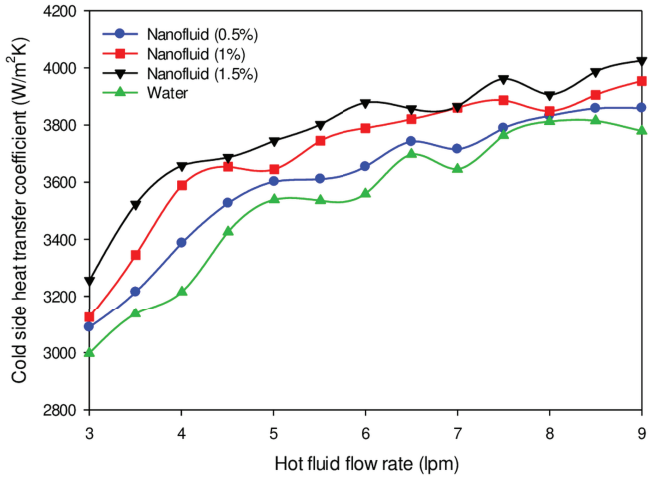

FIG. 9: Change in HTC of the cold side with respect to the flow rate in CFTHE

nanoparticles at 0.5%, 1%, and 1.5% concentration, respectively. However, a maximum enhancement of 5%, 6.5%, and 13% at 0.5%, 1%, and 1.5% nanoparticle concentration, respectively, was achieved.

The effectiveness of heat exchanger is another crucial indicator in analyzing the thermal behavior of the heat exchanger. Variations of the effectiveness in PFTHE and CFTHE via the Reynolds number are illustrated in Figs. 10 and 11. As is seen, using Al_2O_3–SiO_2/deionized water hybrid nanofluids increased the effectiveness in PFTHE and CFTHE in the range of 4–26%. The effectiveness decreased by increasing the Reynolds number as it can be seen in Figs. 10 and 11. The Reynolds number rises with raising flow rate. Moreover, it must be said that fluid heat capacity improves by raising the flow rate, so temperature variation of fluid reduces, thus leading to reduction in the effectiveness. High flow rates of flowing fluid lead to reduction in temperature change because the period of fluid presence inside the system decreases and leads to decrease in the effectiveness of heat exchanger. Similar outcomes for THE effectiveness were achieved by Gomaa et al. (2016, 2017) and Khanlari et al. (2020).

Dimensionless exergy loss changes via the Reynolds number in PFTHE and CFTHE are presented in Figs. 12 and 13. Utilizing Al_2O_3–SiO_2/deionized water hybrid nanofluids in PFTHE and CFTHE decreased dimensionless exergy loss in the range of 5–31%. Moreover, it must be said that in CFTHE the rate of heat transfer is high in comparison with PFTHE. Consequently, the exergy loss in CFTHE will be lower in comparison with PFTHE. This

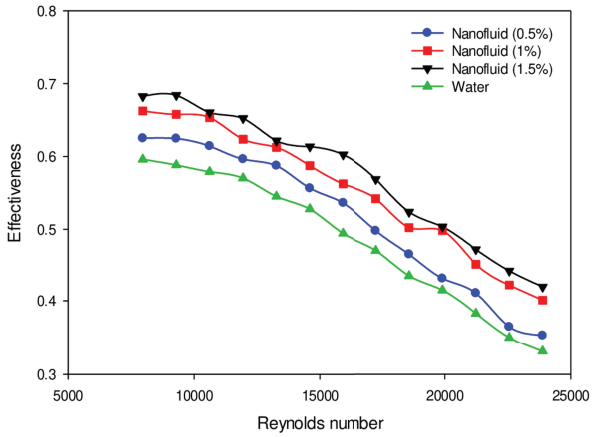

FIG. 10: Effectiveness variation via the Reynolds number in PFTHE

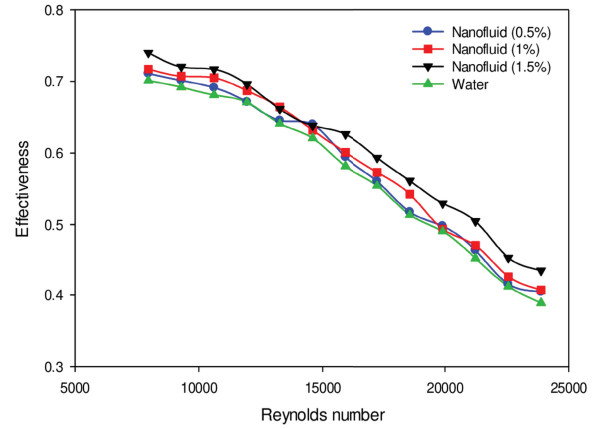

FIG. 11: Effectiveness variation via the Reynolds number in CFTHE

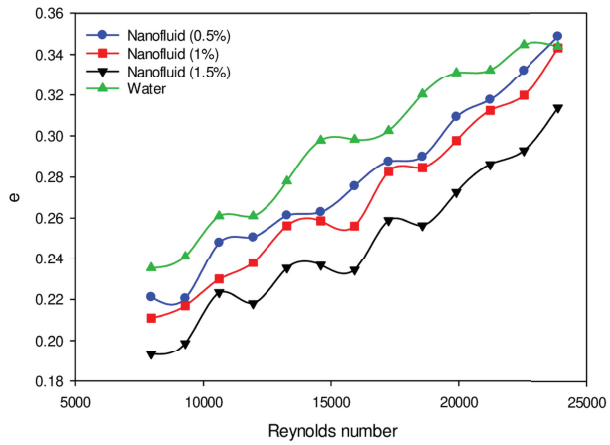

FIG. 12: Change in dimensionless exergy loss with respect to the Reynolds number in PFTHE

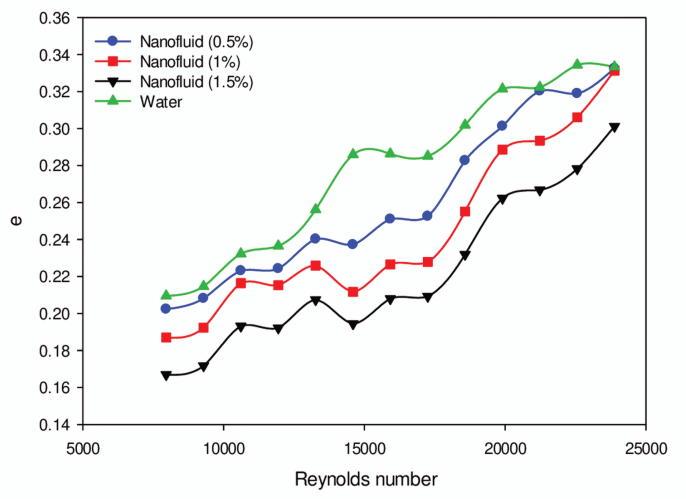

FIG. 13: Change in dimensionless exergy loss with respect to the Reynolds number in CFTHE

fact shows that a high exergy loss of HE is not directly relevant to the rate of heat transfer. The crucial parameter that has important influence on exergy loss is finite temperature variation between hot and cold water. So, it should prevent high local temperature variation among cold and hot fluids in the HE. Similar results for dimensionless exergy loss were obtained by Khanlari et al. (2020).

The experimental results indicated that utilizing Al_2O_3–SiO_2/deionized water hybrid nanofluid at different concentrations on the hot side of the PFTHE and CFTHE enhanced heat transfer notably. Moreover, increasing the nanoparticle ratio from 0.5% to 1.5% caused the increase in thermal efficiency. However, increasing the nanoparticle concentration can cause the sedimentation problem.

4. CONCLUSIONS

In this work, the effects of utilizing Al_2O_3–SiO_2/deionized water hybrid nanofluid at various ratios on the thermal behavior of THE in two different modes were studied. The tests have been performed in various configurations to clarify the behavior of Al_2O_3–SiO_2/deionized water nanofluid. Utilization of this hybrid nanofluid in the PFTHE and CFTHE enhanced heat transfer notably. The highest increments in the OHTC of PFTHE and CFTHE were achieved as 67% and 20%, respectively. Also, the 1.5% nanoparticle concentration showed the best thermal performance in comparison with other concentrations. The experimental outcomes indicated that Al_2O_3–SiO_2/deionized water can be effectively used in THE.

REFERENCES

Afshari, F., Comakli, O., Lesani, A., and Karagoz, S., Characterization of Lubricating Oil Effects on the Performance of Reciprocating Compressors in Air–Water Heat Pumps, *Int. J. Refrig.*, vol. **74**, pp. 503–514, 2017.

Afshari, F., Karagoz, S., Comakli, O., and Ghasemi Zavaragh, H., Thermodynamic Analysis of a System Converted from Heat Pump to Refrigeration Device, *Heat Mass Transf.*, vol. **55**, pp. 281–291, 2019.

Ağbulut, Ü. and Sarıdemir, S., A General View to Converting Fossil Fuels to Cleaner Energy Source by Adding Nanoparticles, *Int. J. Ambient Energy*, 2018. DOI: 10.1080/01430750.2018.1563822

Ağbulut, Ü., Karagöz, M., Sarıdemir, S., and Öztürk, A., Impact of Various Metal-Oxide Based Nanoparticles and Biodiesel Blends on the Combustion, Performance, Emission, Vibration and Noise Characteristics of a CI Engine, *Fuel*, vol. **270**, p. 117521, 2020.

Akhlaghi, E.A., Badali, Y., Altindal, S., and Azizian-Kalandaragh, Y., Preparation of Mixed Copper/PVA Nanocomposites as an Interface Layer for Fabrication of Al/Cu–PVA/*p*-Si Schottky Structures, *Physica B—Condensed Matter*, vol. **546**, pp. 93–98, 2018.

Akyürek, E.F., Gelis, K., Şahin, B., and Manay, E., Experimental Analysis for Heat Transfer of Nanofluid with Wire Coil Turbulators in a Concentric Tube Heat Exchanger, *Results Phys.*, vol. **9**, pp. 376–389, 2018.

Anoop, K., Cox, J., and Sadr, R., Thermal Evaluation of Nanofluids in Heat Exchangers, *Int. Commun. Heat Mass Transf.*, vol. **49**, pp. 5–9, 2013.

Badali, Y., Azizian-Kalandaragh Y., Akhlaghi, E.A., and Altindal S., Ultrasound Assisted Method for Preparation of Ag_2S Nanostructures: Fabrication of Au/Ag_2S–PVA/*n*-Si Schottky Barrier Diode and Exploring Their Electrical Properties, *J. Electronic Mater.*, vol. **49**, pp. 444–453, 2020.

Badali, Y., Koçyiğit, S., Aytimur, A., Altindal, Ş., and Uslu, I., Synthesis of Boron and Rare Earth Stabilized Graphene Doped Polyvinylidene Fluoride (PVDF) Nanocomposite Piezoelectric Materials, *Polymer Compos.*, vol. **40**, pp. 3623–3633, 2019.

Bahiraei, M., Mazaheri, N., and Rizehvandi, A., Application of a Hybrid Nanofluid Containing Graphene Nanoplatelet–Platinum Composite Powder in a Triple-Tube Heat Exchanger Equipped with Inserted Ribs, *Appl. Therm. Eng.*, vol. **149**, pp. 588–601, 2019.

Çiftçi, E. and Sözen, A., Heat Transfer Enhancement in Pool Boiling and Condensation Using h-BN/DCM and SiO_2/DCM Nanofluids: Experimental and Numerical Comparison, *Int. J. Numer. Methods Heat Fluid Flow*, 2020. DOI: 10.1108/HFF-02-2020-0113

Giwa, S.O., Sharifpur, M., and Meyer, J.P., Experimental Study of Thermo-Convection Performance of Hybrid Nanofluids of Al_2O_3–MWCNT/Water in a Differentially Heated Square Cavity, *Int. J. Heat Mass Transf.*, vol. **148**, p. 119072, 2020.

Gomaa, A., Halim, M.A., and Elsaid, A.M., Enhancement of Cooling Characteristics and Optimization of a Triple Concentric-Tube Heat Exchanger with Inserted Ribs, *Int. J. Therm. Sci.*, vol. **120**, pp. 106–120, 2017.

Gomaa, A., Halim, M.A., and Elsaid, A.M., Experimental and Numerical Investigations of a Triple Concentric-Tube Heat Exchanger, *Appl. Therm. Eng.*, vol. **99**, pp. 1303–1315, 2016.

Heyhat, M.M., Abdi, A., and Jafarzad, A., Performance Evaluation and Exergy Analysis of a Double Pipe Heat Exchanger under Air Bubble Injection, *Appl. Therm. Eng.*, vol. **143**, pp. 582–593, 2018.

Hormozi, F., ZareNezhad, B., and Allahyar, H.R., An Experimental Investigation on the Effects of Surfactants on the Thermal Performance of Hybrid Nanofluids in Helical Coil Heat Exchangers, *Int. Commun. Heat Mass Transf.*, vol. **78**, pp. 271–276, 2016.

Kabeel, A.E., El Maaty, T.A., and El Samadony, Y., The Effect of Using Nano-Particles on Corrugated Plate Heat Exchanger Performance, *Appl. Therm. Eng.*, vol. **52**, pp. 221–229, 2013.

Karagöz, M., Ağbulut, Ü., and Sarıdemir, S., Waste to Energy: Production of Waste Tire Pyrolysis Oil and Comprehensive Analysis of Its Usability in Diesel Engines, *Fuel*, vol. **275**, p. 117844, 2020.

Karagöz, S., Afshari, F., Yildirim, O., and Comakli, O., Experimental and Numerical Investigation of the Cylindrical Blade Tube Inserts Effect on the Heat Transfer Enhancement in the Horizontal Pipe Exchangers, *Heat Mass Transf.*, vol. **53**, pp. 2769–2784, 2017.

Karimi, A. and Afrand, M., Numerical Study on Thermal Performance of an Air-Cooled Heat Exchanger: Effects of Hybrid Nanofluid, Pipe Arrangement and Cross Section, *Energy Convers. Manage.*, vol. **164**, pp. 615–628, 2018.

Kaya, M., Gürel, A.E., Ağbulut, Ü., Ceylan, I., Çelik, S., Ergün, A., and Acar, B., Performance Analysis of Using CuO–Methanol Nanofluid in a Hybrid System with Concentrated Air Collector and Vacuum Tube Heat Pipe, *Energy Convers. Manage.*, vol. **199**, p. 111936, 2019.

Khanlari, A., Yılmaz Aydın, D., Sözen, A., Gürü, M., and Variyenli, H.I., Investigation of the Influences of Kaolin-Deionized Water Nanofluid on the Thermal Behavior of Concentric Type Heat Exchanger, *Heat Mass Transf.*, vol. **56**, pp. 1453–1462, 2020.

Mansoury, D., Ilami Doshmanziari, F., Kiani, A., Chamkha, A.J., and Sharifpur, M., Heat Transfer and Flow Characteristics of Al_2O_3/Water Nanofluid in Various Heat Exchangers: Experiments on Counterflow, *Heat Transf. Eng.*, vol. **41**, pp. 220–234, 2020.

Ozdemir, M.B. and Ergun, M.E., Experimental and Numerical Investigations of Thermal Performance of Al_2O_3/Water Nanofluid for a Combi Boiler with Double Heat Exchangers, *Int. J. Numer. Methods Heat Fluid Flow*, vol. **29**, pp. 1300–1321, 2019.

Saba, F., Ahmed, N., Khan, U., and Mohyud-Din, S.T., A Novel Coupling of (CNT−Fe_3O_4/H_2O) Hybrid Nanofluid for Improvements in Heat Transfer for Flow in an Asymmetric Channel with Dilating/Squeezing Walls, *Int. J. Heat Mass Transf.*, vol. **136**, pp. 186–195, 2019.

Sajid, M.U., and Ali, H.M., Thermal Conductivity of Hybrid Nanofluids: A Critical Review, *Int. J. Heat Mass Transf.*, vol. **126**, pp. 211–234. 2018.

Shahrul, I.M., Mahbubul, I.M., Saidur, R., and Sabri, M.F.M., Experimental Investigation on Al_2O_3–W, SiO_2–W and ZnO–W Nanofluids and Their Application in a Shell and Tube Heat Exchanger, *Int. J. Heat Mass Transf.*, vol. **97**, pp. 547–558, 2016.

Sonawane, S.S., Khedkar, R.S., and Wasewar, K.L., Study on Concentric Tube Heat Exchanger Heat Transfer Performance Using Al_2O_3–Water Based Nanofluids, *Int. Commun. Heat Mass Transf.*, vol. **49**, pp. 60–68, 2013.

Soylu, S.K., Atmaca, I., Asiltürk, M., and Doğan, A., Improving Heat Transfer Performance of an Automobile Radiator Using Cu and Ag Doped TiO_2 Based Nanofluids, *Appl. Therm. Eng.*, vol. **157**, p. 113743, 2019.

Sözen, A., Gürü, M., Khanlari, A., and Çiftçi, E., Experimental and Numerical Study on Enhancement of Heat Transfer Characteristics of a Heat Pipe Utilizing Aqueous Clinoptilolite Nanofluid, *Appl. Therm. Eng.*, vol. **160**, p. 114001, 2019.

Sözen, A., Gürü, M., Menlik, T., Karakaya, U., and Çiftçi, E., Experimental Comparison of Triton X-100 and Sodium Dodecyl Benzene Sulfonate Surfactants on Thermal Performance of TiO_2–Deionized Water Nanofluid in a Thermosiphon, *Exp. Heat Transf.*, vol. **31**, pp. 450–469, 2018.

Sözen, A., Variyenli, H.I., Özdemir, M.B., and Gürü, M., Improving the Performance of Parallel and Cross-Flow Concentric Tube Heat Exchangers Using Fly-Ash Nanofluid, *Heat Transf. Eng.*, vol. **37**, pp. 805–813, 2016a.

Sözen, A., Variyenli, H.I., Özdemir, M.B., Gürü, M., and Aytaç, I., Heat Transfer Enhancement Using Alumina and Fly Ash Nanofluids in Parallel and Cross-Flow Concentric Tube Heat Exchangers, *J. Energy Inst.*, vol. **89**, pp. 414–424, 2016b.

Variyenli, H.I., Experimental and Numerical Investigation on Heat Transfer Enhancement in Plate Heat Exchanger Using Fly Ash Nanofluid, *Heat Transf. Res.*, vol. **50**, pp. 1477–1494, 2019.

Zufar, M., Gunnasegaran, P., Kumar, H.M., and Ng, K.C., Numerical and Experimental Investigations of Hybrid Nanofluids on Pulsating Heat Pipe Performance, *Int. J. Heat Mass Transf.*, vol. **146**, p. 118887, 2020.